

Effects of Envelope Corners on Building Thermal Performance

Gerson H. dos Santos, gerson.santos@pucpr.br

Nathan Mendes, nathan.mendes@pucpr.br

Pontifical Catholic University of Parana – PUCPR/CCET

Thermal Systems Laboratory -LST

Rua Imaculada Conceição, 1155, Curitiba – PR – 80215-901 – Brazil

Abstract. *In order to analyze the effects of building hygrothermal envelope corners on room air temperature and humidity, a three-dimensional model was developed to calculate the coupled heat and moisture transfer through building envelopes. The presented methodology is based on the Philip and De Vries model, using thermophysical properties and transport coefficients highly dependent on moisture content and temperature. First, sensitivity analyses of time step and grid refinement are carried out in terms of room air temperature and humidity. A lumped transient approach for the room air domain has been considered. To conclude, multidimensional corner effects for a simple geometry are presented for different materials.*

Keywords: *building hygrothermal simulation, corner effects*

1. INTRODUCTION

Buildings (residential, commercial and public) are greatly responsible for the total consumption of electricity, in a worldwide context. Only in Brazil, they are responsible for at least 46% (BEN, 2006), which progressively motivates energy conservation studies for promoting building energy efficiency. In this context, many computer simulation tools have been developed (Crawley et al., 2005) to evaluate energy performance of buildings from the early-stage sketches to the complex existing buildings. Nevertheless, building energy simulation tools do not consider the three-dimensionality nature of heat and mass transfer through building envelopes.

When the multidimensional effect is considered, thermal bridges may play an important role. Thermal bridges appear in places where the envelope changes its geometry (ex: corners) or composition or both. Thermal bridge is used to define each part of the building envelope where there is a local increase of heat flux density and a decrease or increase of internal surface temperatures. When surface temperatures decrease, condensation occurs when moist air is cooled down below its dew-point temperature. This condensation can promote the germination and growth of moulds on wall surfaces. Moulds can damage surfaces, causing unpleasant 'musty' odours and health hazards from spores released by the moulds.

The available literature is focused more on the thermal effect only. Brown and Wilson (1963) analyzed the insulation effect with some examples and illustrated factors that influence the thermal performance of the thermal bridges. Hassid (1990) proposed a correction to the one-directional heat transfer algorithms, to account for heat transfer across thermal bridges between parallel elements. In another work, Hassid (1991) implemented into the ESP building energy simulation program this model and showed to be able to predict the order of magnitude of changes due to corner effects and thermal bridges. These effects were not negligible to the prediction of internal surface temperature.

Krarti (1994) described an analytical, two-dimensional steady-state thermal analysis of insulated square corners. The results showed that, even though corner heat loss is reduced with increasing insulation thermal resistance, the risk of moisture damage increases.

Farkh (2001) described the principles and method for the analysis of the bridges, presenting default values, calculated according to the French standards. These values were obtained using linear coefficients for different thermal bridges configurations.

Olsen and Radisch (2002) organized a report about thermal bridges in residential buildings in Denmark, describing the Danish building regulations and standards. This report cites that a Nordic study showed that the transmission loss is likely to increase by 10-50% when more correct calculations of thermal bridges are introduced and, in some cases, this difference can amount up to more than 60% of the total transmission losses, showing definitely how important thermal bridges are, especially for the cold Nordic weathers.

Kosny and Kossecka (2002) showed that in most whole building thermal modeling computer programs like DOE-2, BLAST and ENERGY PLUS, where simplified, one-dimensional, parallel path model is used, the building load estimations may generate serious errors due to the thermal bridge effects.

As observed in the cited works above, only thermal effects are verified. Therefore, in order to analyze the effects of building hygrothermal envelope corners, a three-dimensional model was developed to calculate the coupled heat and moisture transfer through building envelopes. A 8-m³ cube-shaped building is modeled in order to reduce the computational effort due to grid refinement. For ensuring numerical stability in the present model, the linearized set of equations was obtained by using the finite-volume method and the MultiTriDiagonal-Matrix Algorithm (Mendes *et al.*,

2002) to solve a 3-D model to describe the physical phenomena of heat and mass transfer in porous materials. The heat and moisture transfer was based on the theory of Philip and De Vries (1957), which is one of the most disseminated and accepted mathematical formulation, especially for studying heat and moisture transfer through porous soils, considering both vapor diffusion and capillary migration.

2. MATHEMATICAL MODEL

The physical problem is divided into two domains: building envelope (walls and corners) and room air. At the external and internal surfaces, the heat transfer due to convection was considered as boundary condition.

2.1. Envelope Domain

The governing equations, based on the theory of Philip and De Vries (1957), to model heat and mass transfer through porous media, are given by Eqs. (1) and (2). The energy conservation equation is written in the form

$$\rho_0 c_m (T, \theta) \frac{\partial T}{\partial t} = \nabla \cdot (\lambda (T, \theta) \nabla T) - L(T) (\nabla \cdot \mathbf{j}_v) \quad (1)$$

and the mass conservation equation as

$$\frac{\partial \theta}{\partial t} = -\nabla \cdot \left(\frac{\mathbf{j}}{\rho_l} \right), \quad (2)$$

where ρ_0 is the solid matrix density (m^3/kg), c_m , the mean specific heat ($\text{J}/\text{kg K}$), T , temperature ($^\circ\text{C}$), λ , thermal conductivity ($\text{W}/\text{m K}$), L , latent heat of vaporization (J/kg), θ , volumetric moisture content (m^3/m^3), j_v , vapor flow ($\text{kg}/\text{m}^2 \text{K}$), j , total flow ($\text{kg}/\text{m}^2 \text{K}$) and ρ_l the water density (kg/m^3).

The total 3-D vapor flow (\mathbf{j}) - given by summing the vapor flow (\mathbf{j}_v) and the liquid flow (\mathbf{j}_l) - can be described as

$$\begin{aligned} \frac{\mathbf{j}}{\rho_l} = & - \left(D_T (T, \theta) \frac{\partial T}{\partial x} + D_\theta (T, \theta) \frac{\partial \theta}{\partial x} \right) \mathbf{i} - \left(D_T (T, \theta) \frac{\partial T}{\partial y} + D_\theta (T, \theta) \frac{\partial \theta}{\partial y} \right) \mathbf{j} \\ & - \left(D_T (T, \theta) \frac{\partial T}{\partial z} + D_\theta (T, \theta) \frac{\partial \theta}{\partial z} \right) \mathbf{k} \end{aligned} \quad (3)$$

with $D_T = D_{Tl} + D_{Tv}$ and $D_\theta = D_{\theta l} + D_{\theta v}$, where D_{Tl} is the liquid phase transport coefficient associated to a temperature gradient ($\text{m}^2/\text{s K}$), D_{Tv} , vapor phase transport coefficient associated to a temperature gradient ($\text{m}^2/\text{s K}$), $D_{\theta l}$, liquid phase transport coefficient associated to a moisture content gradient (m^2/s), $D_{\theta v}$, vapor phase transport coefficient associated to a moisture content gradient (m^2/s), D_T , mass transport coefficient associated to a temperature gradient ($\text{m}^2/\text{s K}$) and D_θ , mass transport coefficient associated to a moisture content gradient (m^2/s). The hydraulic conductivity was ignored.

The external and internal surfaces boundary condition can be mathematically expressed as:

$$\left(\lambda (T, \theta) \frac{\partial T}{\partial y} \right)_{x=0,H} + (L(T) j_v)_{x=0,H} = h_\infty (T_\infty - T_{x=0,H}) + L(T) h_{m,\infty} (\rho_{v,\infty} - \rho_{v,x=0,H}). \quad (4)$$

Similarly, the mass balance at the internal and external surfaces is written as

$$\left(D_\theta (T, \theta) \frac{\partial \theta}{\partial y} + D_T (T, \theta) \frac{\partial T}{\partial y} \right)_{x=0,H} = \frac{h_{m,\infty}}{\rho_l} (\rho_{v,\infty} - \rho_{v,x=0,H}), \quad (5)$$

where $h_{\infty}(T_{\infty} - T_{x=0,H})$ represents the heat exchanged by convection with the external and internal air respectively, described by the surface conductance h_{∞} and $L(T)h_{m,\infty}(\rho_{v,\infty} - \rho_{v,x=0,H})$, the phase-change energy term. The mass convection coefficient by $h_{m,\infty}$, which is related to h_{∞} by the Lewis' relation.

Equations 4 and 5 show a vapor concentration difference, $\Delta\rho_{v,\infty}$, on their right-hand side. This difference is between the porous surface and air and is normally determined by using the values of previous iterations for temperature and moisture content, generating additional numerical instability. To prevent the instability created by this source term, Mendes *et al.*, 2002 presented a procedure to calculate the vapor flow, independently of previous values of temperature and moisture content. In this way, the term ($\Delta\rho_v$) was linearized as a linear combination of temperature and moisture content, viz.,

$$(\rho_{v,\infty} - \rho_v(s)) = M_1(T_{\infty} - T(s)) + M_2(\theta_{\infty} - \theta(s)) + M_3, \quad (6)$$

where

$$M_1 = A \frac{M}{\mathfrak{R}} \phi ;$$

$$M_2 = \frac{M}{\mathfrak{R}} \left(\frac{P_s(s)}{T(s)} \right)^{prev} \left(\frac{\partial \phi}{\partial \theta(s)} \right)^{prev} ;$$

$$M_3 = \frac{M}{\mathfrak{R}} \left[\left(\frac{P_s(s)}{T(s)} \right)^{prev} R(\theta^{prev}(s)) + \phi_{\infty} (R(T_{\infty}) - R(T^{prev}(s))) \right]$$

In the equations above, the index (s) represents the surface on contact with air and (∞) the air far from that surface, R is a residual function of $\left(\frac{P_s}{T} \right)$, P_s , saturated pressure (Pa), \mathfrak{R} , universal gas constant (J/kmol K), M , molecular mass (kg/kmol), ϕ , relative humidity, *prev*, previous iteration and A is the straight-line coefficient from the approximation(2)

2.2. Internal Air Domain

The present work uses a dynamic model for the analysis of hygrothermal behavior of a room. Thus, a lumped formulation for both temperature and water vapor mass is adopted. Equation (7) describes the energy conservation equation applied to a control volume that involves the room air, which is submitted to loads of conduction, convection and infiltration:

$$\dot{E}_t + \dot{E}_g = \rho_{air} c_{air} V_{air} \frac{dT_{int}}{dt}, \quad (7)$$

where:

\dot{E}_t energy flow that crosses the room (W)

\dot{E}_g internal energy generation rate (W)

ρ_{air} air density (kg/m³)

c_{air} specific heat of air (J/kg-K)

V_{air} room volume (m³)

T_{int} room air temperature (°C)

The term \dot{E}_t , on the energy conservation equation, includes loads associated to the building envelope (sensible and latent heat) and infiltration.

The sensible heat released by the building envelope is calculated as

$$Q_S(t) = \sum_{i=1}^n h_{\text{int}} A_i [T_{i,x=H}(t) - T_{\text{int}}(t)] \quad (8)$$

for the sensible conduction load and as

$$Q_L(t) = \sum_{i=1}^n L(T_{x=H}(t)) h_{m,\text{int}} A_i [\rho_{v,\text{int}}(t) - \rho_{v,i}(t)] \quad (9)$$

for the latent load.

In Eq. 8 A_i represents the area of the i -th surface (m^2), h_{int} the internal convection heat transfer coefficients ($\text{W}/\text{m}^2 \text{K}$), $T_{i,x=H}(t)$ the temperature at the i -th internal surface of the building ($^{\circ}\text{C}$), $T_{\text{int}}(t)$ the room air temperature ($^{\circ}\text{C}$), n , is the number of control volumes of the internal surface discretized by using the finite-volume method. In Eq. 9, L represents the vaporization latent heat (J/kg), $h_{m,\text{int}}$, the internal mass convection coefficient (m/s), $\rho_{v,\text{int}}$, the room air water vapor density (kg/m^3) and $\rho_{v,i}$ the water vapor density at the i -th internal surface of the building (kg/m^3).

In terms of water vapor mass balance, contributions were considered from infiltration and building envelope. In this way, the lumped formulation becomes:

$$\dot{m}_{\text{inf}} (W_{\text{ext}} - W_{\text{int}}) + \sum_{i=1}^n h_D A_i [W_{v,i} - W_{\text{int}}] = \rho_{\text{air}} V_{\text{air}} \frac{dW_{\text{int}}}{dt} \quad (10)$$

where \dot{m}_{inf} is the mass flow by ventilation (kg/s), W_{ext} the external humidity ratio ($\text{kg water}/\text{kg dry air}$), W_{int} is the internal humidity ratio ($\text{kg water}/\text{kg dry air}$), h_D is the massa transfer coefficient ($\text{kg}/\text{m}^2\text{s}$), A_i represents the area of i -th control volumes of the internal surface (m^2), $W_{v,i}$ is the humidity ratio of each control volume ($\text{kg water}/\text{kg dry air}$), ρ_{air} , the air density ($\text{kg dry air}/\text{m}^3$) and V_{air} the room volume (m^3).

Santos and Mendes (2004) presented and discussed different numerical methods used to integrate the differential governing equations in the air domain (Eqs. 7 and 10), showing the results in terms of accuracy and computer run time.

3. SIMULATION PROCEDURE

For the simulation, the building was modeled as a “box” ($2\text{m} \times 2\text{m} \times 2\text{m}$) to reduce the computational efforts due to grid refinement (see results section). Moreover, this box has exactly the same dimensions as the box that is being built now (www.pucpr.br/1st) for the purposes of results validation.

In Figs. 2-6, the mortar properties were considered for 0.10 m thick walls. Contact resistance and discontinuity between the materials were not considered and a low infiltration rate of 0.1 l/s was adopted in the all cases. The convection boundary condition was imposed in all the surfaces.

The differential equations of the building envelope were discretized by using the finite-volume method (Patankar, 1980), with a central difference scheme, a uniform grid and a fully-implicit approach. The solution of the set of algebraic equations was obtained by using the MultiTriDiagonal-Matrix Algorithm (Mendes *et al.*, 2002).

The thermophysical properties of the steel corner were gathered from Incropera (1998) and considered constant as shown in Tab. 1.

Table 1: Thermophysical Properties (Incropera, 1998).

Material	λ (W/mK)	ρ (kg/m^3)	c_p (J/kgK)
Steel	63.9	7832	434

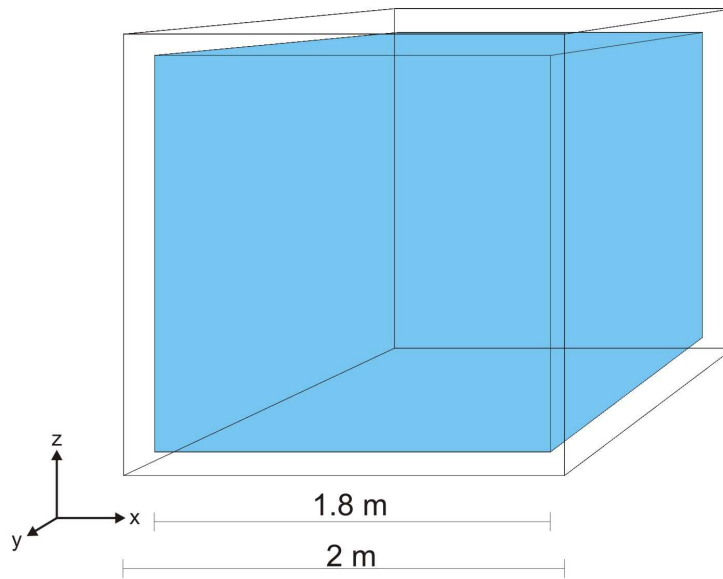


Figure 1. Dimensions of the cubic box under analysis.

The mortar and concrete properties were obtained in Perrin (1985). The dry-basis properties are shown in Table 2.

Table 2: Dry-basis properties of mortar and concrete.

Material	ρ_0 (m ³ /kg)	c_m (J/kg K)	porosity
Mortar	2050	932	0.18
Concrete	849	921.1	0.0408

Except for the sensitivity analyses case where grid refinement and time step were analyzed, an amount of 173,530 nodes were used.

The external climate was represented by Eqs. 11 and 12 for temperature and relative humidity. It was considered a temperature of 20 °C with a daily variation of 5°C. For the external relative humidity, a daily variation between 50 % and 70 % was considered.

$$T_{ext} = 20 + 5 \text{sen} \left(\pi + \frac{\pi t}{43200} \right) \quad (11)$$

$$\phi_{ext} = 0.60 - 0.10 \text{sin} \left(\pi + \frac{\pi t}{43200} \right) \quad (12)$$

4. RESULTS

In Figs. 2-6, a temperature of 10 °C and a relative humidity of 20 % were considered as initial conditions for the envelope and room air. Sensitivity analyses of time step and grid refinement are shown in Figs 2 and 3, in terms of room air temperature and relative humidity. The envelope was discretized with 4 and 8 sections and time steps of 30 s and 120 s were utilized. The results were compared to those obtained by the PowerDomus Program (Mendes et al, 2003). This software was developed and validated to model the one-dimensional coupled heat and moisture transfer in multi-zone buildings. In this way, asymmetries (sun, rain, shadow effects) at the external surfaces in the present study were not generated.

In Figs. 2 and 3, a good agreement between the results obtained by using the program PowerDomus and data obtained in the present study can be seen when the time step decreases. The CPU time requirement was equal to the simulated time, for 8 sections and 30 s of the time step in a computer with Intel Processor 3.4 GHz and 4 GB of RAM, showing how time consuming is the three-dimensional simulation of heat and moisture transfer through porous building envelopes.

Comparing the mesh refinement, better results for the coarse grid were observed, once the more refined the mesh the lower the time step so that the dimensionless Fourier number - strongly present in the source term of the conservation equations - would increase the residual errors due to the interactions between the three dimensions for heat and mass transfer, and, additionally, the three-dimensional nature of the phenomenon would be artificially decoupled by the use of a one-dimensional numerical solver. In this way, the algorithm may bring wrong results when mesh refinement and time step are not adopted to assure the lowest numerical inaccuracies.

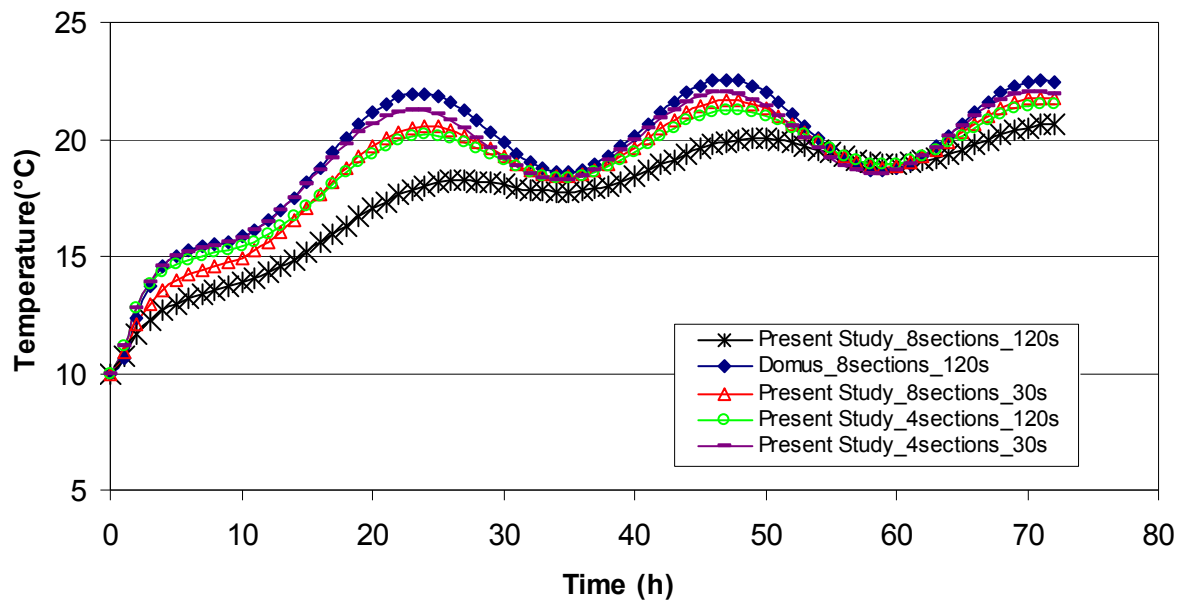


Figure 2. Internal temperature evolution.

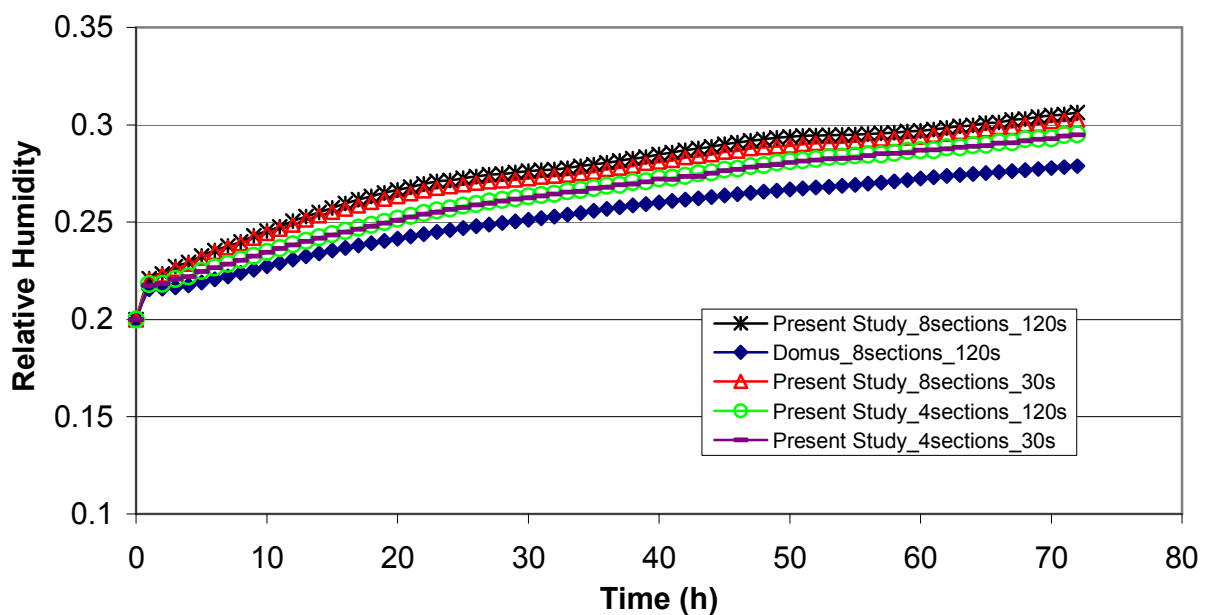


Figure 3. Relative humidity evolution .

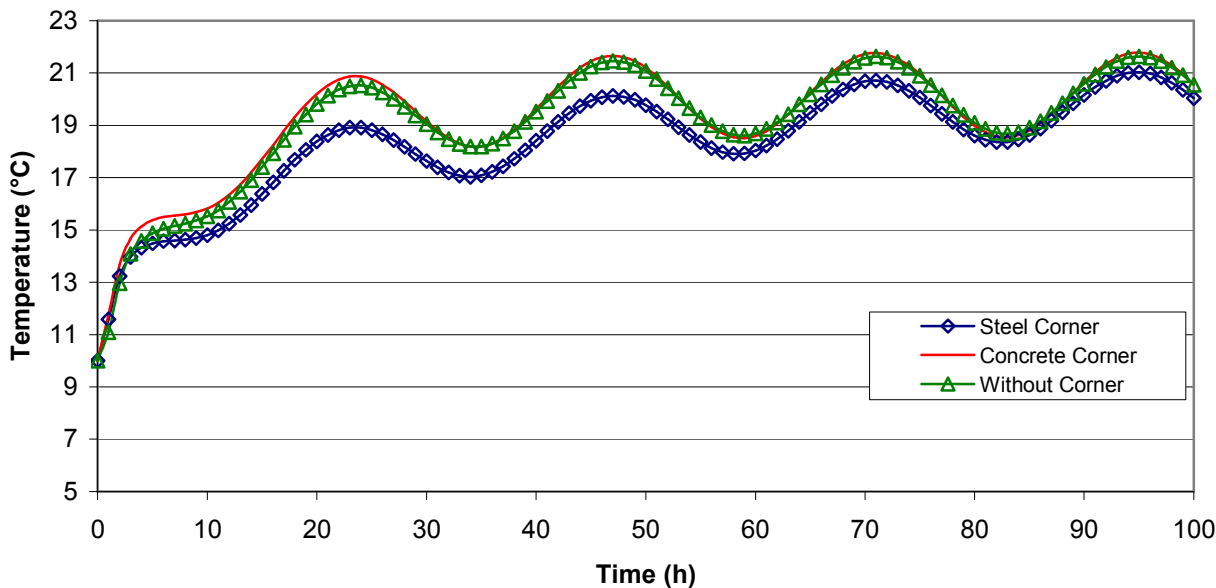


Figure 4. Internal temperature evolution.

In Fig. 4, a 2°C temperature difference is noticed between the values when a steel corner is utilized. This effect is minimized by infiltration effect after some hours. An insignificant difference between the concrete corner and without corner was observed. This fact was attributed to high higrothermal capacitance of the concrete and due to the short simulation period.

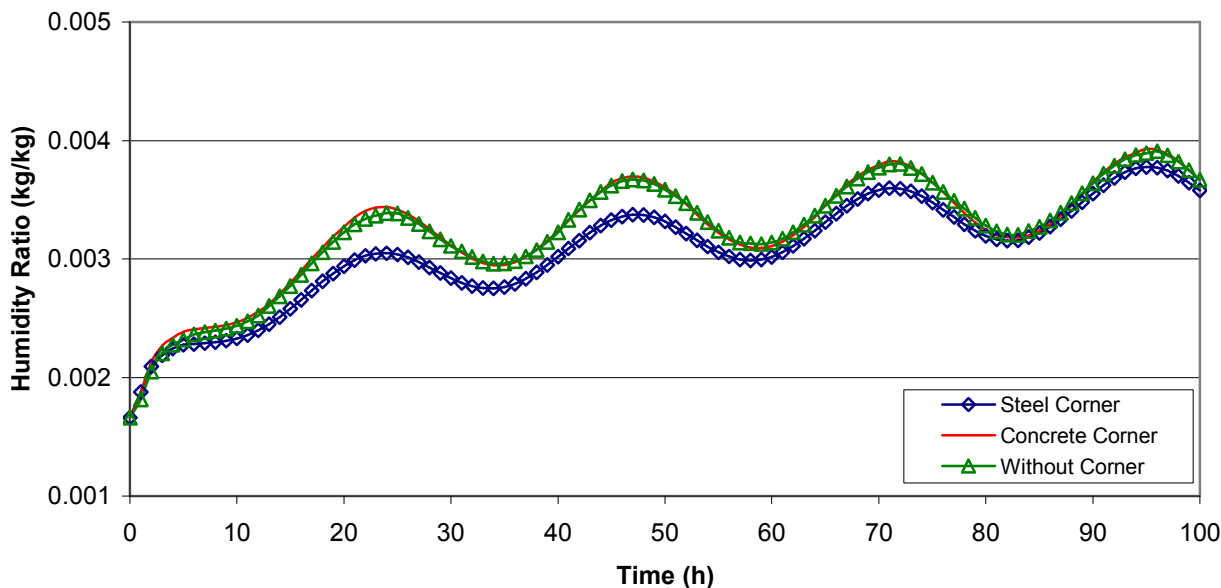


Figure 5. Internal humidity ratio evolution.

The internal humidity ratio observed in Fig. 5 has a similar behavior for the temperature. A 0.0005 kg/kg humidity ratio difference is noticed between the values when a steel corner is utilized. The moisture effect could be higher if longer simulation periods had been considered.

The hygrothermal effects of the corners are mainly observed in temperature and moisture content profiles in the envelope (Figs. 6 and 7). In Fig. 6, the temperature decrease around the corner region is verified. There is in that region an increase of heat flow density and condensation is likely to occur.

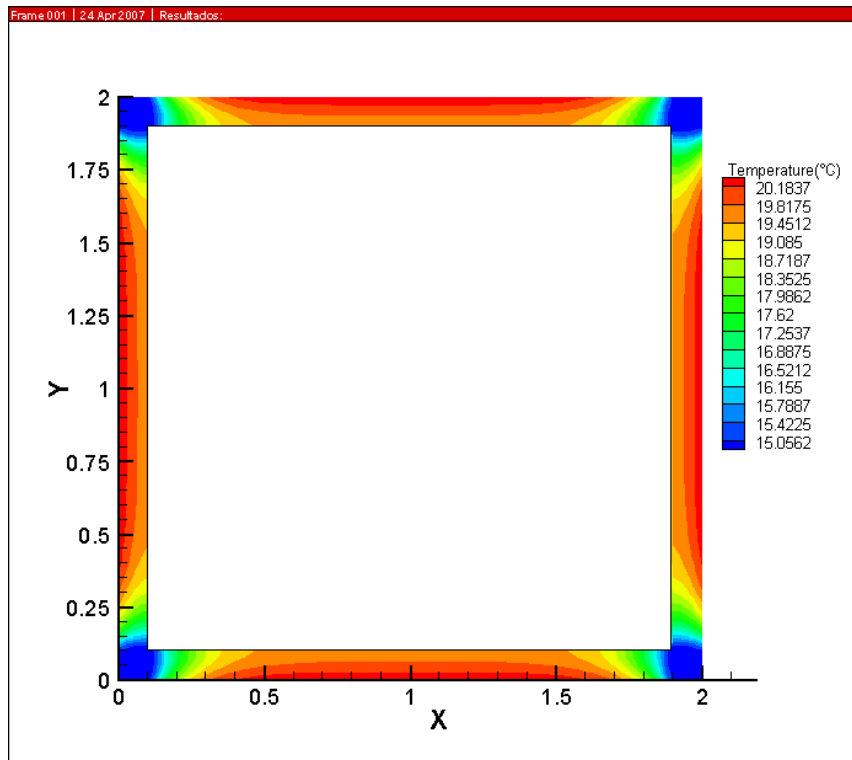


Figure 6. Temperature (°C) profile within the envelope after 20 hours of simulation (steel corner and mortar envelope).

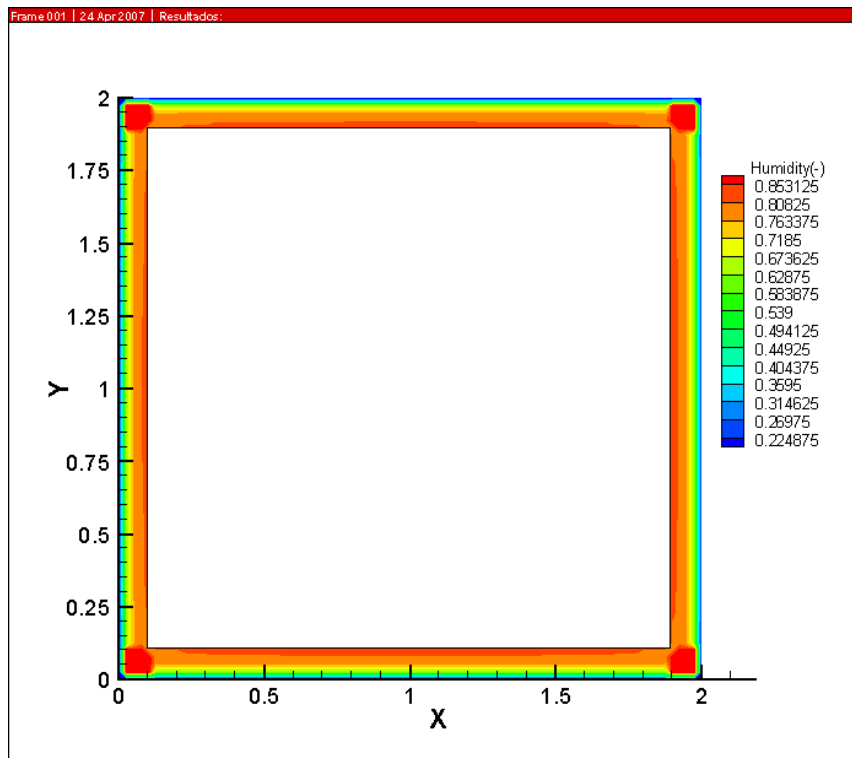


Figure 7. Relative humidity (-) profile within the envelope after 240 hours of simulation (concrete corner and mortar envelope).

In Fig. 7, a temperature of 10 °C and a relative humidity of 90 % were considered as initial conditions. A more humid region was found in the corner after 240 hours of simulation. In this case, the more capacitive material was used in the corner (concrete). Due to the presence of higher moisture content, this region can promote for instance mould growth.

4. CONCLUSION

This paper has presented some effects of building envelope corners on room air temperature and humidity using a three-dimensional heat and moisture transfer model. First, a sensitivity analysis was carried out to show the influence of time step and grid refinement.

In the analysis of the corner effect, a difference of 2°C and 0.0005 kg/kg were noticed in the first hours of simulation, when the room structure corners are made of steel.

Due to the fact that simulations were quite time consuming, the corner effects on the room air temperature and humidity were evaluated only for 100 hours. Those effects were better observed along a cross section of the envelope temperature and moisture content profiles. In the corner region, a decrease on the temperature (steel bridge) was observed. However, when the concrete was utilized in the corner, this region became more humid than the envelope itself after 240 h of simulation.

For future works, a real building geometry with ground contact will be simulated. In the building envelope, multi-dimensional effects will be analyzed applying asymmetries as sun, rain and shadow for longer simulation periods.

5. REFERENCES

- BEN - 2006. Balanço Energético Nacional 2006: Ano base 2005, Ministério de Minas e Energia. Relatório final, 188 p.
- Brown, W. P., Wilson, A. G., 1963, "CBD-44. Thermal Bridges in Buildings"
<http://irc.nrc-cnrc.gc.ca/pubs/cbd/cbd044_e.html>.
- Farkh, S., 2001, "Ponts Thermiques", Th-U, Fascicule 5/5, 133 p.
- Hassid, S., 1990, "Thermal Bridges Across multilayer Walls: An Integral Approach", Building and Environment, Vol. 25, pp. 143-150.
- Hassid, S., 1991, "Algorithms for Multi-Dimensional Heat Transfer in Buildings", International IBPSA Conference. International Building Performance Simulation Association., pp. 9-13.
- Incropera F.P., 1998, "Fundamentos de Transferência de Calor e de Massa", 4th ed., LTC Editora.
- Krarti, M., 1994, "Heat Loss and moisture Condensation for Wall Corners", Energy Conversion and Management, Vol. 35, N. 8, pp. 651-659.
- Mendes, N., Oliveira, R. C. L. F., Santos, G. H., 2003, "DOMUS 2.0: A Whole-Building Hygrothermal Simulation Program, Building Simulation 2003, Eindhoven. Eighth International IBPSA Conference, Vol.2, pp.863 – 869.
- Mendes, N., Philippi, P. C., Lamberts, R., 2002, "A new mathematical method to solve highly coupled equations of heat and mass transfer in porous media" International Journal of Heat and Mass Transfer, Vol. 45, pp. 509-518.
- Olsen, L., Radisch, N., 2002, "Thermal Bridges in Residential Buildings in Denmark", Danish Technological Institute, ISBN – 80-902689-6-X, 19 p.
- Patankar, S.V., 1980, "Numerical Heat Transfer and Fluid Flow", Hemisphere Publishing Corporation.
- Perrin, B., 1985, "Etude des Transferts Couplés de Chaleur et de Masse dans des Matériaux Poreux Consolidés non Saturés Utilisés en Génie Civil", Thèse Docteur d'Etat, Université Paul Sabatier de Toulouse, Toulouse, France.
- Philip, J. R., de Vries, D. A., 1957, "Moisture movement in porous media under temperature gradients" Trans. Am. Geophysical Union, Vol. 38, pp. 222-232.
- Santos, G. H., Mendes, N., 2004, "Analysis of Numerical Methods and Simulation Time Step Effects on the Prediction of Building Thermal Performance", Applied Thermal Engineering, Vol. 24, pp.1129-1142.

6. RESPONSIBILITY NOTICE

The authors are the only responsible for the printed material included in this paper.